

RESEARCH ARTICLE

Open Access



# Update of the year 2019 modeling emission inventory in China

Seoyeon Kim<sup>1</sup>, Jinseok Kim<sup>2</sup>, Hyejung Hu<sup>1,3</sup>, Meongdo Jang<sup>1,3</sup>, Jae-Bum Lee<sup>4</sup>, Sung Chul Hong<sup>4</sup>, Okgil Kim<sup>4</sup> and Jung-Hun Woo<sup>1,3\*</sup> 

## Abstract

Using updated emission inventories can enhance the accuracy of air quality forecast models. Given China's rapid economic growth and Korea's geographical and meteorological position on the windward side of China, updating China's emission inventory has become particularly crucial for Korea's air quality modeling. This study aimed to develop an updated version of China's Emission Inventory in Comprehensive Regional Emissions for Atmospheric Transport Experiments version 3 for the base year of 2019 (CREATEv3 (YR 2019)). To achieve this goal, we utilized the Chinese emission inventory of CREATEv3 for the base year of 2015 (CREATEv3 (YR 2015)) as a framework to incorporate the latest Chinese emission data from the Multi-resolution Emission Inventory Model for Climate and Air Pollution Research for the base year of 2019 (MEIC COVID-19 (YR 2019)) and update the inventory. The updated China's annual emissions are now reflected in CREATEv3 (YR 2019), and the amounts are as follows: 132 Tg for CO, 21 Tg for NO<sub>x</sub>, 8 Tg for SO<sub>2</sub>, 7 Tg for PM<sub>2.5</sub>, 9 Tg for NH<sub>3</sub>, and 28 Tg for volatile organic compound (VOC). By comparing previous Chinese emission inventories with the updated inventory developed in this study, it was found that SO<sub>2</sub>, NO<sub>x</sub>, VOC, and NH<sub>3</sub> emissions were decreased. Therefore, using the updated inventory seemingly reduces the impact of China's fine dust on Korea. By comparing emissions by pollutant and region in China using CREATEv3 (YR 2019), it was found that regions with high emissions of targeted pollutants strongly correlated with major industries operating in those areas. This study is expected to provide insights into China's emission changes in 2019 and support air quality forecasting.

**Keywords** Emission inventory, Air quality forecast, Comprehensive regional emission inventory for atmospheric transport experiment (CREATE), Multi-resolution emission inventory model for climate and air pollution research (MEIC)

## 1 Introduction

Recently, there has been an increasing interest in and concern regarding the impact of air pollution on human health and the environment. To address this concern, the National Institute of Environmental Research has provided official air quality forecasts since August 2013, which have been published on its website (<https://www.airkorea.or.kr/web/>). Air quality forecasting in Korea utilizes numerical models to generate forecasts, and the final forecast level is determined by forecaster decisions, as described by Jang et al. (2014). Lee et al. (2016) analyzed the accuracy of the fine dust forecast from August 2013 to February 2014, which was the testing period for the fine dust forecast. The accuracy

\*Correspondence:

Jung-Hun Woo  
jwoo@konkuk.ac.kr

<sup>1</sup> Department of Technology Fusion Engineering, Konkuk University, Seoul 05029, South Korea

<sup>2</sup> Department of Advanced Technology Fusion, Konkuk University, Seoul 05029, South Korea

<sup>3</sup> Civil and Environmental Engineering, College of Engineering, Konkuk University, Seoul 05029, South Korea

<sup>4</sup> Air Quality Forecasting Center, National Institute of Environmental Research (NIER), Incheon 22689, South Korea



of the entire period was found to be 71.8%. Among these results, the forecast accuracy for fine dust analyzed only for days with high concentrations was 33.3%. Bae et al. (2017) highlighted the issue that the level of pollution experienced by citizens and the forecast differ significantly. They emphasized the need for research to enhance the accuracy of air quality forecasts. To improve forecast accuracy, it is essential to enhance the accuracy of the air quality model, which depends significantly on emissions data, as noted by Lee et al. (2014). Thus, using the latest emission inventory as input data is critical for producing accurate air quality forecasts.

To forecast the air quality in South Korea, emission inventories from South Korea and neighboring countries are necessary. Comprehensive Regional Emission Inventory for Atmospheric Transport Experiment version 1 for the base year of 2010 (CREATEv1 (YR 2010)) was developed by Woo et al. (2020) and can be used for air quality modeling in South Korea. This inventory included emissions of both anthropogenic and biogenic pollutants from the East Asian region and was created based on data from 2010. Additionally, CREATEv1 (YR 2010) was upgraded to create CREATEv3 (YR 2015) (NIER, 2021), which updated the base year to 2015. Emission inventories for East Asia have been updated in various studies. For instance, the Korea-United States air quality field campaign emission inventory version 5 for the base year of 2016 (KORUSv5 (YR 2016)) was jointly created in 2016 by the National Institute of Environmental Research and NASA based on CREATEv1 (YR 2010) to support international cooperative air quality research observation (NIER, 2017). The Long-range Transboundary Air Pollutant in Northeast Asia for the base year 2017 of (LTP (YR 2017)) emission inventory was created for the base year of 2017 based on CREATEv1 (YR 2010) (NIER, 2019) with a collaborative agreement between Korea, China, and Japan (NIER, 2019).

Continuous updates to the emission inventory of East Asia are necessary to improve the accuracy of South Korea's air quality models. This research was conducted to update China's emission inventory, which is relevant for air quality modeling in South Korea. This is because South Korea, which is located geographically and meteorologically downwind of China, is significantly affected by air pollutants from China (NIER, 2017; Kim et al., 2023). In particular, rapid economic growth and urbanization have occurred in China, resulting in significant emission changes. Recently, as various air quality improvement policies have been implemented, air pollutants have rapidly reduced (Li et al., 2021). Therefore, it is necessary to use emission inventories that reflect these circumstances in air quality modeling.

To prepare an emission inventory for China that adequately reflects the current circumstances, the following process was carried out. Firstly, China's emission data that best reflect the recent emission tendencies in China were investigated to update China's emissions in CREATEv3 (YR 2015). The latest inventory for China was created using the Multi-resolution Emission Inventory Model for Climate and Air Pollution Research (MEIC, n.d.; <http://meicmodel.org/lang=en>). In their research, Zheng et al. (2021) assessed China's emission changes due to the COVID-19 lockdown. The researchers collected activity data from 2019 and 2020, comparing emissions before and after the lockdown. The resulting emission inventory based on 2019 data is referred to as the Multi-resolution Emission Inventory Model for Climate and Air Pollution Research for the base year of 2019 (MEIC COVID-19 (YR 2019)), representing normal emissions without the impact of lockdown measures. This inventory was selected for our research. It was considered more suitable than the MEIC emission inventory for the base year 2020, which excludes the impact of COVID-19. The structure of MEIC COVID-19 (YR 2019) differed from that of CREATEv3 (YR 2015); therefore, a matching process was performed to reflect recent emissions. Consequently, the latest Chinese emission inventory, CREATEv3 (YR 2019), was developed.

Next, the updated Chinese emissions in CREATEv3 (YR 2019) were reviewed from several aspects. First, CREATEv3 (YR 2019) and MEIC COVID-19 (YR 2019) were compared to ensure the latest data was appropriately reflected. CREATEv3 (YR 2019) was also compared with previous emission inventories, including CREATEv3 (YR 2015), KORUSv5 (YR 2016), and LTP (YR 2017), to review changes in emission trends in China. During this process, the emissions of each pollutant were analyzed for each region in China using CREATEv3 (YR 2019) to understand the emission characteristics of each pollutant according to the industrial structure of each region in China. Second, emissions for the air quality model input data were created using CREATEv3 (YR 2019). Sparse Matrix Operator Kernel Emissions for Asia (SMOKE-Asia; Woo et al., 2012) were used for this purpose. The researchers then identified whether CREATEv3 (YR 2019), which was created as a result of this research, could be used as the input data for an air quality prediction model.

## 2 Data collection

### 2.1 Northeast Asia emission inventories based on CREATE

In this study, several previously established emission inventories for East Asia were used, including CREATEv3 (YR 2015), KORUSv5 (YR 2016), and LTP (YR 2017). The focus of this research was to update China's emissions in

CREATEv3 (YR 2019) with the base year of 2019, using the emissions data from CREATEv3 (YR 2015) with the base year of 2015. After the update, the newly established inventory was compared with previous inventories to analyze the characteristics of recent emission changes in China.

CREATEv3 (YR 2015) is a comprehensive emission inventory that includes both anthropogenic and biogenic emissions for 13 different types of pollutants: CO<sub>2</sub>, CH<sub>4</sub>, NO<sub>x</sub>, N<sub>2</sub>O, PM<sub>10</sub>, PM<sub>2.5</sub>, SO<sub>2</sub>, volatile organic compound (VOC), NH<sub>3</sub>, CO, BC, OC, and mercury. An inventory is a bottom-up approach that identifies and distinguishes approximately 300 different types of emission sources and fuels; updates to relevant databases (DBs), such as activity rates, can be easily performed. CREATEv3 (YR 2015) has been utilized as an emission inventory in various modeling studies, including air quality modeling (Woo et al., 2020). The total emissions of each pollutant in each sector in China, calculated using CREATEv3 (YR 2015), are shown in Table 1.

KORUSv5 (YR 2016) was updated with 2016 emissions based on CREATEv1 (YR 2010) (NIER, 2017), and numerous studies have been conducted by Korean and international researchers on its application in modeling and aerial observation data analysis (e.g., Choi et al., 2019; Simpson et al., 2020). The LTP (YR 2017) collected emission data in 2017 under the agreement of South Korea, China, and Japan, and these emissions

data were applied to analyze the long-distance dispersion of air pollutants (NIER, 2019).

### 2.2 Recent emission inventories for China

MEIC is an emission inventory for China developed and managed by Tsinghua University. The MEIC provides an emission inventory for eight major air pollutants, CO, SO<sub>2</sub>, NO<sub>x</sub>, NMVOC, NH<sub>3</sub>, PM<sub>2.5</sub>, OC, and BC, including more than 700 emissions sources since 1990 in China. The emissions data were categorized into five large sectors: power, industry, residential, transport, and agriculture.

To assess the effect of the recent COVID-19 lockdown, MEIC COVID-19 (Zheng et al., 2021) has been created and provided. To compare emissions in 2020 during the lockdown to those in the previous year, activity data from 2019 and 2020 were collected to estimate anthropogenic emissions in China and create an emission inventory. In this research, the MEIC COVID-19 (YR 2019) emission data were utilized as the emission inventory before the lockdown to reflect the normal emissions characteristics, and China emissions in CREATEv3 (YR 2015) were updated accordingly. Table 2 presents the emissions of various pollutants from each emission source in China based on the MEIC COVID-19 (YR 2019).

**Table 1** CREATEv3 (YR 2015) emissions by sector and pollutant in China (unit: Gg/year)

Pollutant\sector	CO	SO <sub>2</sub>	NO <sub>x</sub>	VOC	NH <sub>3</sub>	PM <sub>10</sub>	PM <sub>2.5</sub>
Power	567	3274	4645	11,519	82	1103	568
Industry	92,837	14,404	9349	624	2317	5489	2742
Residential	43,636	3503	936	4435	83	3851	3539
Transport	15,717	243	8371	2487	40	725	610
Agriculture	806	-	-	408	11,272	843	305
Other	12,077	45	1034	2508	1107	1944	1771
Total	165,640	21,468	24,335	21,981	14,901	13,956	9535

**Table 2** MEIC COVID-19 (YR 2019) emissions by sector and pollutant in China (unit: Gg/year)

Pollutant/sector	CO	SO <sub>2</sub>	NO <sub>x</sub>	VOC	NH <sub>3</sub>	PM <sub>2.5</sub>
Power	5178	1345	3893	58	-	229
Industry	46,455	4481	9009	18,343	272	2913
Residential	54,794	2494	803	4675	319	2817
Transport	22,159	117	7228	3970	47	436
Agriculture	-	-	-	-	8,323	-
Total	128,586	8437	20,933	27,046	8962	6390

### 3 Methods

#### 3.1 Research framework

Figure 1 presents an overview of the study. The main focus of this research was to update the CREATEv3 (YR 2015) emission inventory to CREATEv3 (YR 2019) by incorporating the latest Chinese emission inventory data from MEIC COVID-19 (YR 2019). A matching process was performed to accommodate structural differences in MEIC COVID-19 (YR 2019) and CREATEv3 (YR 2015). In order to validate the accuracy of the updated emission inventory, the China emission inventory in CREATEv3 (YR 2019) was compared to the actual China emission data in 2019 as represented by MEIC COVID-19 (YR 2019). Additionally, the emissions in China from CREATEv3 (YR 2019) were compared with those from the previously established CREATEv3 (YR 2015), KORUSv5 (YR 2016), and LTP (YR 2017) to review recent emission changes. During this process, the emissions of each pollutant in each region of China were analyzed to identify the emission characteristics according to the industrial structure of each region. In addition, the CREATEv3 (YR 2019) emission inventory was used as input data for SMOKE-Asia to create Chemical Transport Model-ready (CTM-ready) emissions. This allows the inventory to be used in atmospheric models to predict air quality.

#### 3.2 Developing China emissions for CREATEv3 (YR 2019)

The method used to update CREATEv3 (YR 2015) with emissions from MEIC COVID-19 (YR 2019) is simple and straightforward. CREATEv3 (YR 2015) calculated emissions considering both anthropogenic and biogenic emissions, but CREATEv3 (YR 2019) calculated emissions targeting only anthropogenic emissions. The projection factors are calculated based on the ratio of

emissions in MEIC COVID-19 (YR 2019) to the base inventory of CREATEv3 (YR 2015) for each pollutant, region, and sector. These factors were multiplied by the emissions from CREATEv3 (YR 2015) for each pollutant, region, and sector, generating an updated CREATEv3 (YR 2019) inventory. This method ensures that the latest emission information is incorporated into the inventory while maintaining consistency with the previous inventory.

$$P.F_{P,R,S} = \frac{Em_{(MEIC\ COVID-19(Yr.2019))P,R,S}}{Em_{(CREATEv3(Yr.2015))P,R,S}} \quad (1)$$

$P.F_{P,R,S}$ : projection factors of pollutants, regions, and sectors.

$Em_{(MEIC\ COVID-19(Yr.2019))P,R,S}$ : Controlled emissions of each pollutant, region, and sector [MEIC COVID-19 (YR 2019)].

$Em_{(CREATEv3(Yr.2015))P,R,S}$ : Controlled emissions of each pollutant, region, and sector [CREATEv3 (YR 2015)].

Several factors should be considered before using Eq. (1). As shown in Table 3, the two inventories differed slightly in terms of included regions, emission source sectors, and pollutant types. Regarding the difference in the regional distinction, MEIC COVID-19 (YR 2019), unlike CREATEv3 (YR 2015), does not include Hong Kong and Macao. Additionally, the Tier 1 emission source category in MEIC COVID-19 (YR 2019) does not include an “other sector,” and the PM<sub>10</sub> emissions are not provided. After reviewing the emissions for each sector in Tables 1 and 2, it was found that only NH<sub>3</sub> emissions were included in the emissions from the agricultural sector in MEIC COVID-19 (YR 2019), and NH<sub>3</sub> emissions were not provided in the power sector. Therefore, the emissions omitted in MEIC COVID-19 (YR 2019) must be included, and

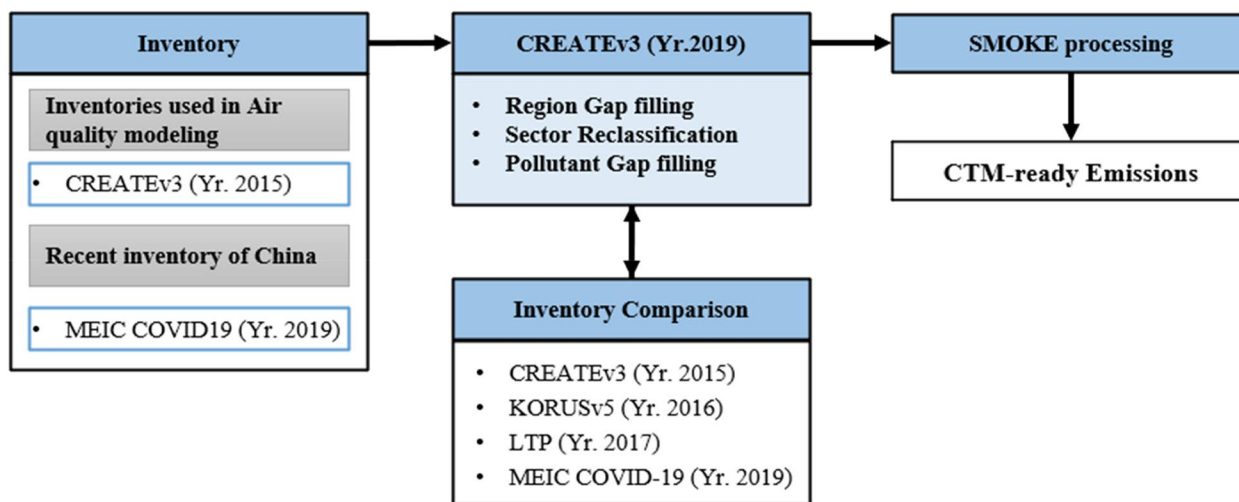


Fig. 1 Research flow chart

**Table 3** Summary of CREATEv3 (YR 2015) and MEIC COVID-19 (YR 2019) format

Inventory	Region	Sector		Pollutant
		Tier1	Tier2	
CREATEv3 (YR 2015)	32 Province	Power, industry, transport, residential, agriculture, <b>other</b>	<b>186 Sub-sector</b>	CO, SO <sub>2</sub> , NO <sub>x</sub> , VOC, NH <sub>3</sub> , PM <sub>2.5</sub> , <b>PM<sub>10</sub></b>
MEIC COVID-19 (YR 2019)	31 Province (w/o. Hong Kong and Makau) <sup>a</sup>	Power, industry, transport, residential, agriculture	-	CO, SO <sub>2</sub> , NO <sub>x</sub> , VOC, NH <sub>3</sub> , PM <sub>2.5</sub>

<sup>a</sup> The emissions from Hong Kong and Macau were calculated by grouping them into regions

the emission source classification sectors must be unified with CREATEv3 (YR 2015).

*Region gap filling* The emissions from Hong Kong and Macao were included in CREATEv3 (YR 2015) but not in MEIC COVID-19 (YR 2019). To calculate the emissions from Hong Kong and Macao in CREATEv3 (YR 2019), the projection factor (rate of change in emissions) of Guangdong Province, which is adjacent to Hong Kong and Macao, was used. Specifically, the projection factor obtained from the increase in Guangdong emissions in MEIC COVID-19 (YR 2019) compared to the emissions in Guangdong in CREATEv3 (YR 2015) was applied to the emissions from Hong Kong and Macao in CREATEv3 (YR 2015) to calculate their emissions in CREATEv3 (YR 2019).

*Sector reclassification* To address the issue of inconsistent classification systems caused by the absence of the “other sector” category in MEIC COVID-19 (YR 2019), the sources of emissions classified as “other sector” in

CREATEv3 (YR 2015) were reclassified by referring to Tier 2, which provides a more detailed classification system. In CREATEv3 (YR 2015), the “other sector” was reclassified into power, industry, transport, residential, agriculture, and other sectors, as shown in Table 4. Of note, the “solvent-use sector” was added as a new category.

Emissions from the newly added solvent-use sector were not included in MEIC COVID-19 (YR 2019), so they were estimated by referring to MEICv1.2 2010, the 2010 emission inventory of MEIC. As summarized in Table 5, the data provided by the MEIC homepage do not separately distinguish VOC emissions due to solvent use. However, in a study relevant to an identical inventory (Li et al., 2017), the solvent-use sector was distinguished. Based on the two reference datasets, the ratios of VOC emissions from solvent use in the industrial and residential sectors were determined to be 0.45 and 0.12, respectively. These ratios were applied to MEIC COVID-19 (YR 2019) emissions to calculate emissions from the solvent-use sector.

**Table 4** Reclassification of CREATEv3 (YR 2015) “other sector”

Sector			Assigned Sector
Tier1	Tier2	Description	
Other	D_GASST	Gasoline distribution—service stations	<b>Industry</b>
	D_REFDEP	Gasoline storage & distribution (excl. gas stations)	<b>Industry</b>
	D_REFDEP_S	Gasoline storage & distribution (excl. transport sector)	<b>Industry</b>
	EXD_LQ	Extraction of oil (incl. delivery to terminals)	<b>Industry</b>
	MSW_FOOD	Food and organic waste in MSW	<b>Residential</b>
	MSW_OTH	Waste composition: fraction of other waste in MSW	<b>Residential</b>
	MSW_PAP	Waste composition: fraction of paper in MSW	<b>Residential</b>
	MSW_PLA	Municipal plastic waste	<b>Residential</b>
	MSW_TEX	Waste composition: fraction of textile in MSW	<b>Residential</b>
	MSW_WOOD	Waste composition: fraction of wood in MSW	<b>Residential</b>
	OTH_NH <sub>3</sub> EMISS	Other NH <sub>3</sub> emissions	<b>Agriculture</b>
	OTHER_VOC	Other NMVOC emissions	<b>Solvent use</b>
	WASTE_AGR	Agricultural waste burning	<b>Agriculture</b>

Table 6 provides an example of a VOC emission reclassification procedure in Beijing. To calculate the emissions for the industrial and residential sectors, the original emissions were multiplied by their respective VOC ratios (0.55 and 0.88) obtained from Table 7. This resulted in emissions of 160.5 Gg/year and 38.9 Gg/year, respectively. The resulting value for the solvent-use sector was 135.9 Gg/year. The same process was then applied to all other regions to recalculate VOC emissions by sector and to compute VOC emissions in the solvent-use sector.

**Pollutant gap filling** First, in the case of PM<sub>10</sub> emissions, emissions were estimated in CREATEv3 (YR 2015) but not in MEIC COVID-19 (YR 2019). Therefore, the PM<sub>10</sub> emissions of CREATEv3 (YR 2019) were calculated by applying the ratio of change of PM<sub>2.5</sub> emissions for each region and sector that existed in both CREATEv3 (YR 2015) and MEIC COVID-19 (YR 2019) to the PM<sub>10</sub> emissions of CREATEv3 (YR 2015).

Second, the NH<sub>3</sub> emissions not included in the power sector in MEIC COVID-19 (YR 2019) were estimated based on the value presented in the study by Jang et al.

(2020). The authors of this study reported that NH<sub>3</sub> was emitted as a byproduct of NO<sub>x</sub> reduction when selective catalytic reduction (SCR) and selective non-catalytic reduction (SNCR) systems were installed in the power sector to reduce NO<sub>x</sub> emissions. They also presented the NH<sub>3</sub>/NO<sub>x</sub> ratios of coal-fired and non-coal-fired power plants to determine the NH<sub>3</sub> emissions in the power sector of China. Therefore, in the present study, NH<sub>3</sub> emissions of the power sector were calculated by distinguishing coal and non-coal fuels sector-wise and applying the appropriate regional NH<sub>3</sub>/NO<sub>x</sub> ratio based on fuel classification.

The MEIC COVID-19 (YR 2019) only considered NH<sub>3</sub> emissions for the agricultural sector, as shown in Table 2. However, CREATEv3 (YR 2015) included CO, VOC, PM<sub>10</sub>, and PM<sub>2.5</sub>, in addition to NH<sub>3</sub> for the agricultural sector, as shown in Table 3. Furthermore, SO<sub>2</sub> and NO<sub>x</sub> emissions could be calculated through sector reclassification in CREATEv3 (YR 2015), as described in Sect. 3.2.2. Table 7 illustrates the pollutants and Tier 2 sectors for the agricultural sector in CREATEv3 (YR 2015), indicating that fugitive emissions from livestock and agricultural

**Table 5** VOC emissions by sector in MEIC v1.2 2010 (unit: Gg/year)

Sector\reference	Agriculture	Industry	Power	Transport	Residential	Solvent use
MEIC Website (A)	0	14,286 (100%)	66	2,352	5703 (100%)	-
Li et al. (2017) (B)	0	<b>7878 (55.15%)</b>	66	2,352	<b>5014 (87.92%)</b>	<b>7151</b>
Difference (A-B) <sup>a</sup>	0	<b>6407 (44.85%)</b>	0	0	<b>689 (12.08%)</b>	<sup>b</sup>

<sup>a</sup> VOC emissions due to solvent use among total VOC emissions in a sector

<sup>b</sup> The difference in the total VOC emissions between the two references was 54.2 Gg/year. This discrepancy is thought to be due to the methodology of Li et al. (2017) for estimating sectoral VOC emissions, which may have included some solvent-use emissions from sectors beyond the industrial and residential sectors

**Table 6** Reclassification of Beijing VOC emissions in MEIC COVID-19 (YR 2019) (unit: Gg/year)

	Agriculture	Industry	Power	Transport	Residential	Solvent use
Original	-	291.1 (100%)	1.1	83.3	44.2 (100%)	-
Difference	-	<b>130.5 (44.85%)</b>	0	0	<b>5.3 (12.08%)</b>	-
After reclassification	-	<b>160.5 (55.15%)</b>	1.1	83.3	<b>38.9 (87.92%)</b>	<b>135.9</b>

**Table 7** Sub-sectors and pollutants of the agricultural sector in CREATEv3 (YR 2015)

Sector\pollutant	Tier1	Tier2	Description
NH <sub>3</sub> + PM (NH <sub>3</sub> , PM <sub>10</sub> , PM <sub>2.5</sub> )	Agriculture	AGR_BEEF	Fugitive emissions from livestock (other cattle)
		AGR_COWS	Fugitive emissions from livestock (dairy cattle)
		AGR_PIG	Fugitive emissions from livestock (pigs)
		AGR_POULT	Fugitive emissions from livestock (poultry)
		STH_AGR	Storage & handling of agricultural crops
PM (PM <sub>2.5</sub> , PM <sub>10</sub> )		WASTE_AGR	Agricultural waste burning
All pollutants (CO, SO <sub>2</sub> , NO <sub>x</sub> , VOC, NH <sub>3</sub> , PM <sub>10</sub> , PM <sub>2.5</sub> )			

waste burning also emit pollutants other than NH<sub>3</sub>. Therefore, the ratio of NH<sub>3</sub> emission changes between CREATEv3 (YR 2015) and MEIC COVID-19 (YR 2019) can help estimate China’s emissions of all pollutants in the agricultural sector for CREATEv3 (YR 2019).

### 3.3 Developing CTM-ready emission using CREATEv3 (YR 2019)

In this study, CREATEv3 (YR 2019) was used as the input data for SMOKE-Asia to create CTM-ready emissions. The SMOKE (Sparse Matrix Operator Kernel Emissions), developed by the United States Environmental Protection Agency (U.S. EPA), is a powerful and flexible emission processing system. It was selected as the base system for developing an Asian emissions processing system, SMOKE-Asia. SMOKE-Asia was developed according to the emission inventories and the processing of surrogates based on Asia. The differences between SMOKE and SMOKE-Asia are in temporal allocation and chemical speciation profiles regionalized using resources from Asia-based studies. SOMKE-Asia is a model for generating emission input data suitable for the CTM, such as Comprehensive Air quality Model with extensions (CAMx, n.d.; <https://www.camx.com/>) and Community Multiscale Air Quality (CMAQ, n.d.; <https://www.epa.gov/cmaq>). This approach was developed specifically for emission treatment in Asia. Figure 2 shows a flowchart of the SMOKE-Asia process used in this study. First, the CREATEv3 (YR 2019) emission inventory was

transformed into the one record per line (ORL) data format required by SMOKE-Asia (UNC, 2020). The transformed emission inventory was then input into SMOKE-Asia, and the spatial allocation of emissions for each emission source, temporal allocation of emissions, and chemical speciation of emissions were processed in parallel. Finally, the allocation results were merged to create the CTM-ready emissions.

The framework for emissions processing is shown in Table 8. A spatial allocation process of air pollutant emissions was applied to each region, yielding gridded emissions that were used in the air quality models. The latest overseas geographical data were reflected to proceed with a more precise spatial allocation to construct the database. Temporal allocation is the process of temporal allocation of the inventory, written as annual emissions. To consider emission trends in China over time, the latest data from China were used to create a temporal allocation profile. In this research, processed emissions were created on an hourly basis. Chemical speciation is a process used to generate input data considering photochemical reactions during air quality modeling. Among the chemical mechanism methods, the carbon bond mechanism (CB6; Yarwood et al., 2010) and AEROSol module version 7 (AERO7; Sonntag et al., 2014) chemical species classification were applied, and chemical speciation factors were created for the recent model input. Some of the profiles provided as basic values in SMOKE were enhanced using

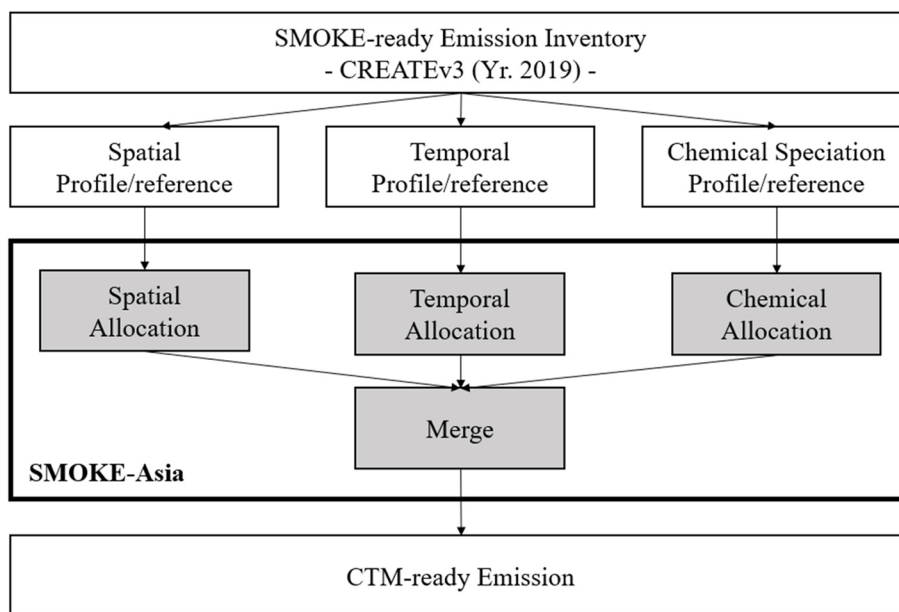


Fig. 2 SMOKE-Asia processing steps

**Table 8** Emission modeling framework

Anthropogenic emission processor	SMOKE-Asia (SMOKE v4.5)
Modeling domain (spatial resolution)	Grid resolution (number of grid): 27000×27000 (174×128) Projection types: lamber conformal conic Projection units: meters Projection alpha value: 30' N Projection beta value: 60' N Projection gamma value: 126' E X-direction projection center in units of the projection: 126' E Y-direction projection center in units of the projection: 38' N X origin in units of the projection: -2,349,000 Y origin in units of the projection: -1,728,000
Temporal resolution	Hourly
Chemical mechanism	VOC: CB6 <sup>a</sup> PM2.5: AERO <sup>b</sup>

<sup>a</sup>Yarwood et al. (2010)

<sup>b</sup>Sonntag et al. (2014)

previous research. In addition, the modeling domain information used to generate emissions per grid, such as grid resolution, number of grids, projection type, projection units, projection alpha value projection beta value, and projection gamma value, is shown in Table 8.

## 4 Results

### 4.1 Emission inventory comparisons

The emissions from China in CREATEv3 (YR 2019) established in this research can be categorized into 32 provincial regions, six Tier 1 emission sources (power, industry, transport, residential, agriculture, and solvent use), and 186 sub-sectors, with emissions for pollutants CO, SO<sub>2</sub>, NO<sub>x</sub>, VOC, NH<sub>3</sub>, PM<sub>10</sub>, and PM<sub>2.5</sub>; Table 9 summarizes the total emissions of each pollutant. CO showed about 131.6 Tg y<sup>-1</sup>, SO<sub>2</sub> 8.5 Tg y<sup>-1</sup>, NO<sub>x</sub> 21.0 Tg y<sup>-1</sup>, VOC 27.7 Tg y<sup>-1</sup>, NH<sub>3</sub> 9.0 Tg y<sup>-1</sup>, PM<sub>10</sub> 10.8 Tg y<sup>-1</sup>, and PM<sub>2.5</sub> 6.9 Tg y<sup>-1</sup>. Further, the emissions by sectors, according to CREATEv3 (2019), indicated that CO accounted for the greatest emissions in the residential sector at 54.8 Tg y<sup>-1</sup>, NH<sub>3</sub> accounted for the greatest emissions in the agricultural sector at 8.3 Tg y<sup>-1</sup>, and in the industrial sector, SO<sub>2</sub> accounted for 4.5 Tg y<sup>-1</sup>, NO<sub>x</sub> 9.0 Tg y<sup>-1</sup>, VOC 10.2 Tg y<sup>-1</sup>, PM<sub>10</sub> 6.0 Tg y<sup>-1</sup>, and PM<sub>2.5</sub> 2.9 Tg y<sup>-1</sup>.

Table 10 shows the pollutant emissions in China according to CREATEv3 (YR 2019), which was developed in this study, and previous emission inventories. Figure 3 shows the same data as bar graphs. Additionally, the values within parentheses in Table 10 refer to the ratios of other inventories based on CREATEv3 (YR 2019). China's emissions contained in CREATEv3 (YR 2019) can be validated through comparison with MEIC COVID-19 (YR 2019) as the current emissions, and the recent emission changes in China can be considered by comparing with inventories with different reference years.

**Table 9** CREATEv3 (YR 2019) emissions by sector and pollutant in China (unit: Gg/year)

	CO	SO <sub>2</sub>	NO <sub>x</sub>	VOC	NH <sub>3</sub>	PM <sub>10</sub>	PM <sub>2.5</sub>
Power	5255	1347	3910	59	83	434	224
Industry	46,462	4493	9024	10,215	272	5999	2916
Residential	54,807	2495	805	4113	320	3073	2818
Transport	22,218	118	7254	3984	48	512	437
Agriculture	2849	14	13	536	8325	761	462
Solvent use	-	-	-	8,831	-	-	-
Total	<b>131,591</b>	<b>8466</b>	<b>21,006</b>	<b>27,737</b>	<b>9047</b>	<b>10,780</b>	<b>6858</b>

**Table 10** China's emissions by pollutant from various inventories (unit: Tg/year)

	CO	SO <sub>2</sub>	NO <sub>x</sub>	VOC	NH <sub>3</sub>	PM <sub>10</sub>	PM <sub>2.5</sub>
CREATEv3 (YR 2019)	131.6 (100%)	8.5 (100%)	21.0 (100%)	27.7 (100%)	9.1 (100%)	10.8 (100%)	6.9 (100%)
MEIC COVID-19 (YR 2019)	128.6 (98%)	8.4 (99%)	20.9 (100%)	27.1 (98%)	9.0 (99%)	-(-)	6.4 (93%)
LTP (YR 2017)	115.5 (88%)	9.4 (111%)	17.1 (81%)	23.8 (86%)	10.1 (111%)	8.8 (81%)	6.7 (97%)
KORUSv5 (YR 2016)	141.9 (108%)	13.4 (158%)	22.5 (107%)	28.4 (103%)	10.3 (113%)	10.8 (100%)	8.1 (117%)
CREATEv3 (YR 2015)	165.6 (126%)	21.5 (253%)	24.3 (116%)	22.0 (79%)	14.9 (164%)	14.0 (130%)	9.6 (139%)



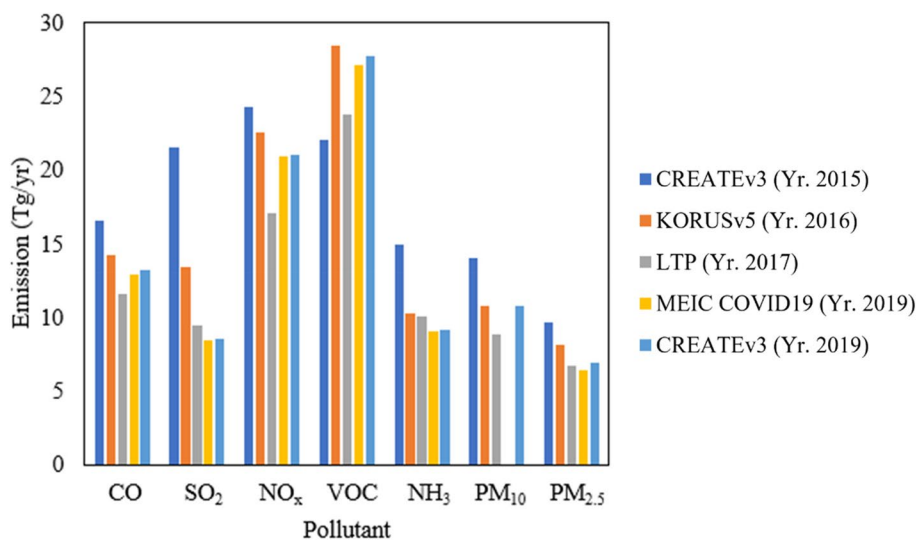


**Fig. 3** Comparison of emission inventories (CO emissions scale: divided by 10)

Comparing Chinese emissions estimated by CREATEv3 (YR 2019) and MEIC COVID-19 (YR 2019) revealed that the two models yielded similar results. The CREATEv3 (YR 2019) emissions showed the following differences compared to MEIC COVID-19 (YR 2019) emissions:  $3.0 \text{ Tg y}^{-1}$  for CO,  $0.1 \text{ Tg y}^{-1}$  for SO<sub>2</sub>,  $0.1 \text{ Tg y}^{-1}$  for NO<sub>x</sub>,  $0.6 \text{ Tg y}^{-1}$  for VOC,  $0.1 \text{ Tg y}^{-1}$  for NH<sub>3</sub>,  $10.8 \text{ Tg y}^{-1}$  for PM<sub>10</sub>, and  $0.5 \text{ Tg y}^{-1}$  for PM<sub>2.5</sub>. The differences between the emissions estimated by CREATEv3 (YR 2019) and MEIC COVID-19 (YR 2019) were primarily attributable to several factors, including the addition of emissions to account for the omission of data from Hong Kong and Macao, the inclusion of other pollutants (excluding NH<sub>3</sub>) resulting from fugitive dust and agricultural waste burning in the agricultural sector, NH<sub>3</sub> emissions generated as a byproduct of NO<sub>x</sub> reduction via SCR and SNCR in the power sector, and an additional calculation of PM<sub>10</sub> emissions. In summary, although we identified differences due to additional emissions and correction of omitted emissions, CREATEv3 (YR 2019) seemed to well reflect MEIC COVID-19 (YR 2019).

In Crippa et al. (2023), most pollutants except VOC and NH<sub>3</sub> show a decreasing trend in China since 2010. LTP (YR 2017) is a government-driven regional collaborative framework between Korea, China, and Japan. The China's inventory for LTP (YR 2017) is believed to apply more stringent emissions control measures from Chinese government. For this reason, emissions from LTP (YR 2017) appeared lower than those from research-driven inventories, such as MEIC COVID-19 (YR 2019) and CREATEv3 (YR 2019). And then, compared to LTP (YR 2017), one of the currently used emissions inventories, Table 10 shows smaller emissions for pollutants other than SO<sub>2</sub> and NH<sub>3</sub>

relative to CREATEv3 (YR 2019). Conversely, compared to KORUSv5 (YR 2016), all pollutants showed higher emissions than those indicated by CREATEv3 (YR 2019); among the pollutants, SO<sub>2</sub> showed 1.5 times higher emissions. The emissions from CREATEv3 (YR 2015) showed higher emissions than CREATEv3 (YR 2019) in all pollutants excluding VOC and about 2.5 times higher emissions for SO<sub>2</sub>.

#### 4.2 Characteristics of China's emissions

Figure 4 shows the emissions of each pollutant in the 32 Chinese provinces. The pollutant emissions from each region in China were compared, and the characteristics of each pollutant emission according to the regional industrial structure were considered. In the figure, the region showing high emissions of CO, SO<sub>2</sub>, NO<sub>x</sub>, VOC, NH<sub>3</sub>, PM<sub>10</sub>, and PM<sub>2.5</sub> is Shandong. This region has the most abundant mineral resources, such as petroleum and natural gas, and is rich in basic resources for industrial development, such as petrochemicals, textiles, and machinery. Additionally, it includes large amounts of arable land, ranking first and second as major agricultural production areas in China. Therefore, Shandong, where heavy chemical industry and agriculture developed, showed high emissions for all pollutants at  $9.16 \text{ Tg y}^{-1}$  of CO,  $0.75 \text{ Tg y}^{-1}$  of SO<sub>2</sub>,  $2.02 \text{ Tg y}^{-1}$  of NO<sub>x</sub>,  $2.45 \text{ Tg y}^{-1}$  of VOC,  $0.63 \text{ Tg y}^{-1}$  of NH<sub>3</sub>,  $0.85 \text{ Tg y}^{-1}$  of PM<sub>10</sub>, and  $0.53 \text{ Tg y}^{-1}$  of PM<sub>2.5</sub>.

CO emissions are generated in urban areas with heavy road traffic, industrial plants that handle chemicals, power generation, organic synthesis, indoor kitchens, and district heating facilities. Therefore, as shown in Fig. 4(a), Hebei and Shandong, where the industrial sector

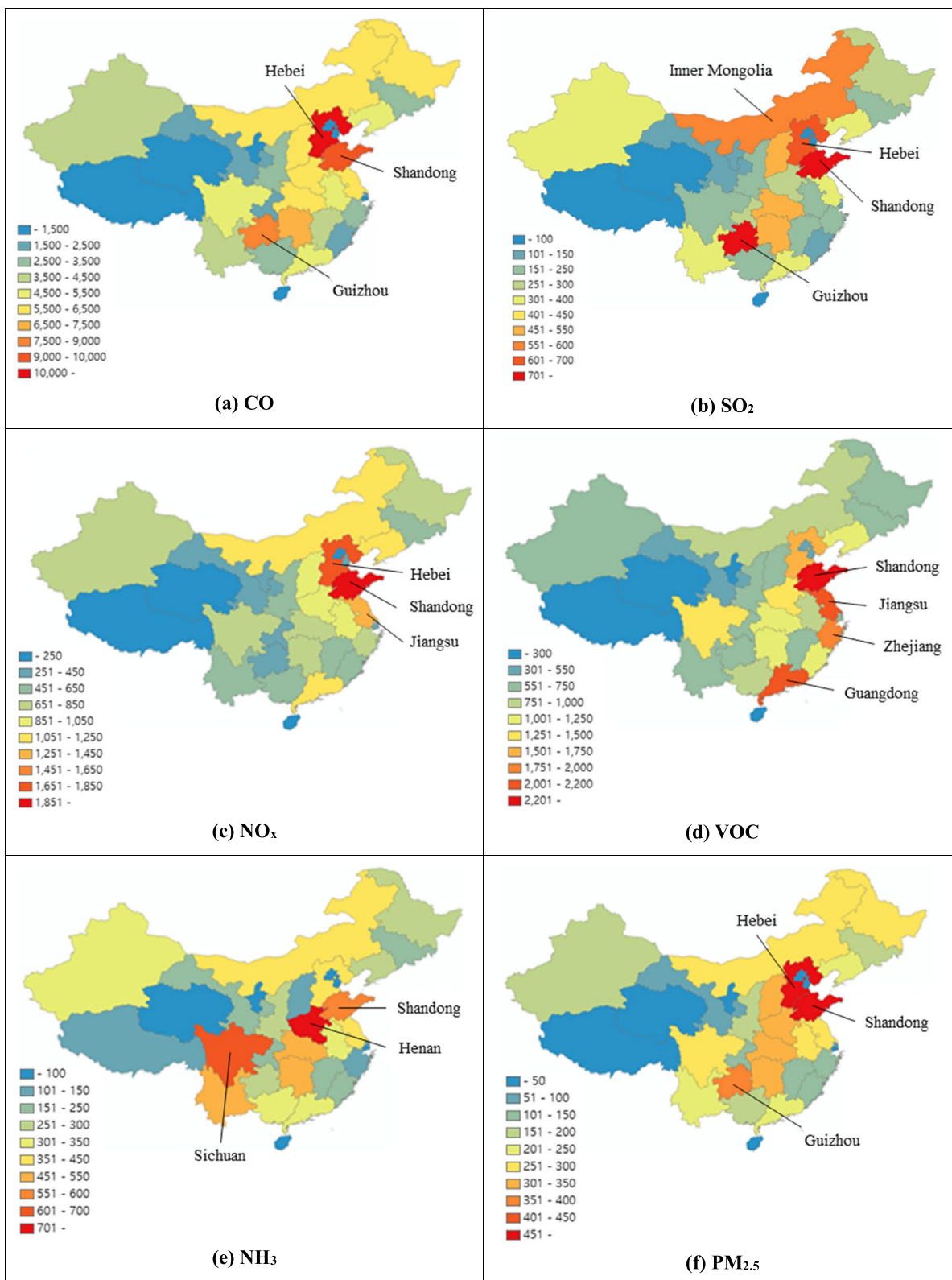


**Fig. 4** CREATEv3 (YR 2019) China emissions region-wise (unit: Gg/year)

(particularly the steel industry) is well-developed because of the abundance of mineral resources such as coal and petroleum, and Guizhou Province, a major energy base in the south, which is rich in mineral resources such as coal and bauxite, showed high emissions at  $11.16 \text{ Tg y}^{-1}$ ,  $9.16 \text{ Tg y}^{-1}$ , and  $8.23 \text{ Tg y}^{-1}$ , respectively. Additionally, these regions showed the highest emissions in the industrial, residential, and transport sectors, whereas emissions from domestic cooking stoves in the residential sector accounted for at least 30% of the total CO emissions.

As shown in Fig. 4(b),  $\text{SO}_2$  emissions in Shandong, Guizhou, Hebei, and Inner Mongolia were  $0.75 \text{ Tg y}^{-1}$ ,  $0.69 \text{ Tg y}^{-1}$ ,  $0.64 \text{ Tg y}^{-1}$ , and  $0.55 \text{ Tg y}^{-1}$ , respectively. Fuels with high sulfur content, such as coal and heavy oil, have higher emissions with an increase in fuel use; therefore, the highest emissions were observed in Guizhou and Hebei, where the industry is well-developed, as well as Inner Mongolia and Shandong, whose industrial sector mainly consists of coal and power generation industries. Among the four regions, the highest emissions were observed in the industrial and power sectors. In Inner Mongolia, total  $\text{SO}_2$  emissions seemed to be relatively high because of the large area ( $1,183,000 \text{ km}^2$ ). However, it was found that emissions were relatively low at  $0.0005 \text{ Gg/year/km}^2$ . Shandong exhibited approximately  $0.0108 \text{ Gg/year/km}^2$ , while Hebei displayed around  $0.0034 \text{ Gg/year/km}^2$ , indicating higher emissions compared to Inner Mongolia.

Figure 4(c) shows that  $\text{NO}_x$  emissions were highest in Shandong, Hebei, and Jiangsu at  $2.02 \text{ Tg y}^{-1}$ ,  $1.72 \text{ Tg y}^{-1}$ , and  $1.41 \text{ Tg y}^{-1}$ , respectively. These three regions have active combustion and manufacturing processes with heavily trafficked; therefore, they all showed high emissions from the industrial and transport sectors. However, the emissions per area were  $0.0316 \text{ Gg/year/km}^2$ ,  $0.0091 \text{ Gg/year/km}^2$ , and  $0.0161 \text{ Gg/year/km}^2$  from Shandong, Hebei, and Jiangsu, respectively. Furthermore, Beijing, as the center of transportation and capital city of China, at  $0.0144 \text{ Gg/year/km}^2$ , showed higher emissions than Hebei, while showing similar emissions with Jiangsu.

VOC are generated and emitted using volatile organic matter rather than fuel combustion; therefore, they are generated during manufacturing in factories of petrochemicals, refineries, paint, and coatings, from storage tanks of petrol stations, and automotive paints and adhesives. Thus, as shown in Fig. 4(d), Guangdong and Zhejiang, whose economies are dominated by light industries, and Jiangsu, where light industries account for at least 50% of the total industrial production costs, showed the highest emissions as  $2.18 \text{ Tg y}^{-1}$ ,  $1.83 \text{ Tg y}^{-1}$ , and  $2.02 \text{ Tg y}^{-1}$ , respectively. In addition, in the case of emissions per area, the highest value was recorded in the Jing-Jin-Ji region (Beijing-Tianjin-Hebei), which is severely

industrialized and has a high population density. In particular, high emissions in this region were attributable to the industrial, solvent-use, transport, and residential sectors.

As shown in Fig. 4(e), the  $\text{NH}_3$  generated during the decomposition of organic and chemical fertilizers or manure was high in Henan (the region with the highest wheat production in China), Sichuan (where grain production, including rice and wheat, is high), and Shandong (whose agricultural sector is well-developed). Thus, all three regions showed the highest emissions in the agricultural sector, with the highest emission being recorded in Henan at  $0.78 \text{ Tg y}^{-1}$ , followed by Sichuan at  $0.66 \text{ Tg y}^{-1}$  and Shandong at  $0.63 \text{ Tg y}^{-1}$ .

$\text{PM}_{2.5}$  is typically produced during fuel combustion owing to incomplete combustion or the presence of ash in the fuel; therefore, significant amounts are generated from solid fuels such as coal, heavy oil, or diesel fuel. Therefore,  $\text{PM}_{2.5}$  is emitted directly from industrial facilities, automobiles, heating, and energy sources. As shown in Fig. 4(f), emissions were high in Shandong, Hebei, and Guizhou, these three regions showed the greatest emissions from the industrial and residential sectors, and emissions were  $0.53 \text{ Tg y}^{-1}$ ,  $0.51 \text{ Tg y}^{-1}$ , and  $0.39 \text{ Tg y}^{-1}$ , respectively. Beijing, the capital of China, showed high emissions due to traffic jams, industrial activity, and coal heating. Accordingly, emissions were primarily generated from industrial activities, such as steel and cement production and coal-fired power plants in Hebei, which surrounds Beijing.

### 4.3 CTM-ready emission results

CREATEv3 (YR 2019), established in this research, was used as the input data for SMOKE-Asia to construct the CTM-ready emissions data. Among the seven pollutants considered as CTM-ready emission data, the results for four pollutants, namely  $\text{SO}_2$ ,  $\text{NO}_x$ , VOC, and  $\text{PM}_{2.5}$ , are shown in Fig. 5. The CTM-ready emissions results from applying the temporal distribution, spatial distribution, and speciation processes. Despite some differences, the CTM-ready emission results show a distribution similar to that of the regional emissions of CREATEv3 (YR 2019), as shown in Sect. 4.2.

As shown in Fig. 5(a), in the case of  $\text{SO}_2$  emissions, the Jing-Jin-Ji region showed high emissions, whereas emissions from Inner Mongolia were low, unlike the regional emission results in Sect. 4.2, where the area was not accounted for. In Fig. 5(b),  $\text{NO}_x$  emissions, which were concentrated in the eastern region, are shown in a specific location where combustion from coal power plants was active. Figure 5(c) shows significant  $\text{PM}_{2.5}$  emissions in the eastern region where Jing-Jin-Ji is located. The gridded emission map of VOC in Fig. 5(c) illustrates the

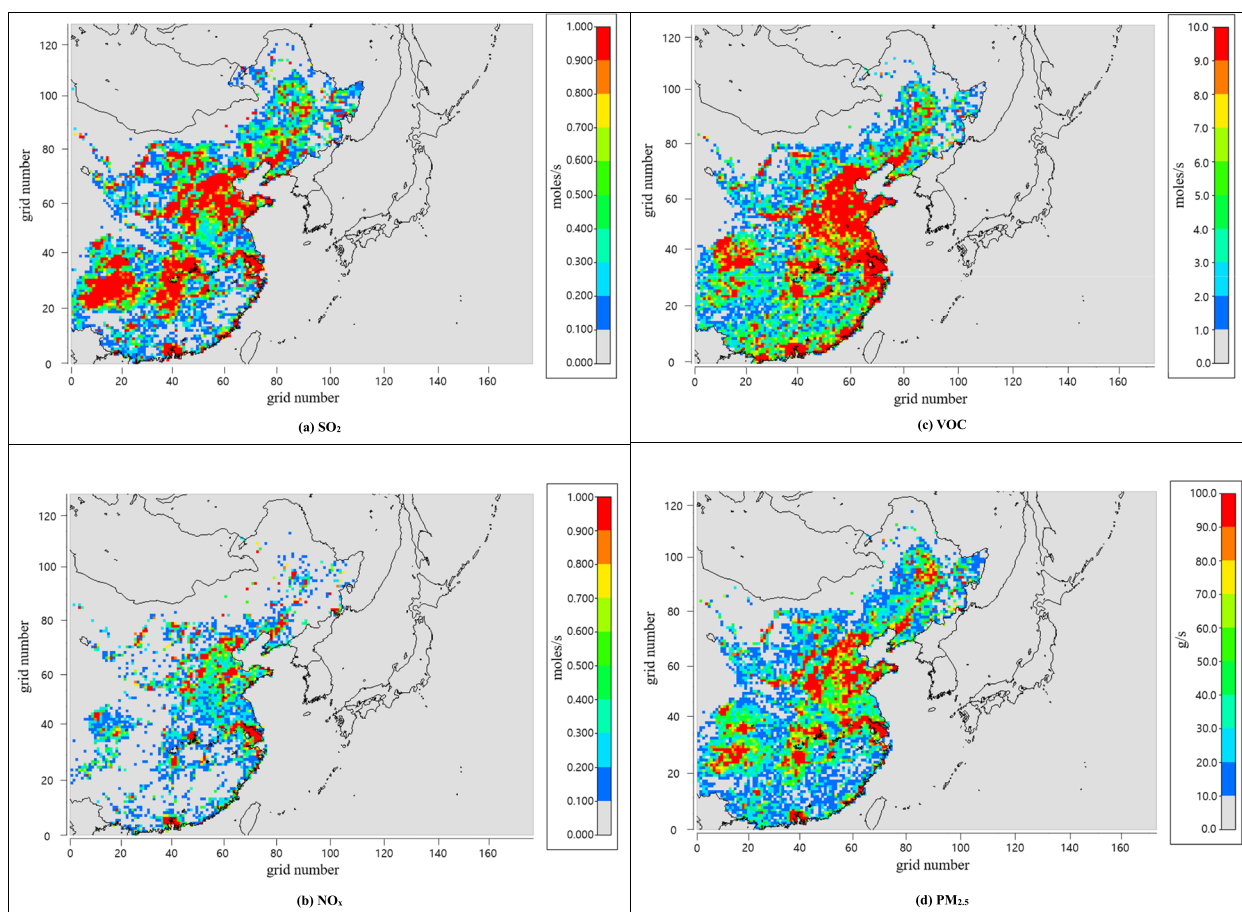


**Fig. 5** CTM-ready emission results using CREATEv3 (YR 2019)

aggregate of values, converted into molar mass through the molecular weights of 19 distinct chemical species. This conversion is undertaken following the transition VOC into the format of the CB6 chemical species mechanism so that it can be used in CTM. Figure 5(d) shows that emissions were high in the Eastern and Southern regions. Thus, the emissions of all the major pollutants ( $\text{SO}_2$ ,  $\text{NO}_x$ , VOC, and  $\text{PM}_{2.5}$ ) were high in the eastern region adjacent to South Korea. In particular, emissions from the industrial regions near Beijing and Shandong and regions near Shanghai (Yangtze River Delta) were significantly high.

## 5 Conclusions

This study aimed to update the emission input data for the air quality forecasting models used in South Korea. Specifically, this study focused on updating China's emission inventory to the base year of 2019. The results were used to generate CTM-ready emissions for forecasting models. To achieve this, (1) the Northeast Asia emissions inventories that were previously used for air

quality prediction models and China's latest inventory were identified. CREATEv3 (YR 2015) China emissions were utilized as the reference inventory, and the latest emissions data of China, MEIC COVID-19 (YR 2019), was used to update and construct China emission inventory in CREATEv3 (YR 2019) with the base year of 2019. (2) While updating the emission inventory, differences between the two inventories for each region, sector, and pollutant were comparatively analyzed. Based on this analysis, relative to the MEIC COVID-19 (YR 2019) inventory, CREATEv3 (YR 2019) included additional emissions data from Hong Kong and Macao, reclassified the other sectors and solvent-use sector, and added emissions for other pollutants (excluding  $\text{NH}_3$ ) in the agricultural sector,  $\text{NH}_3$  emissions in the power sector, and  $\text{PM}_{10}$  emissions. (3) A comparison was made between the CREATEv3 (YR 2019) emission inventory constructed in this study and previous inventories. (4) Additionally, in CREATEv3 (YR 2019), emissions for each pollutant were calculated for each of the 32 provinces and cities in China, and the emission

characteristics were analyzed for each region and industry. (5) Finally, SMOKE-Asia was used to write the CTM-ready emission data and identify the emission characteristics for each major pollutant.

In CREATEv3 (YR 2019), established in this research, China's emissions were categorized into 32 provincial regions and from six sectors, including power, industry, residential, transport, agriculture, and solvent use, and the emissions were computed for seven pollutants: CO, SO<sub>2</sub>, NO<sub>x</sub>, VOC, NH<sub>3</sub>, PM<sub>10</sub>, and PM<sub>2.5</sub>. The total amount of emissions in China for each pollutant from CREATEv3 (YR 2019) was 131.6 Tg yr<sup>-1</sup> for CO, 8.5 Tg yr<sup>-1</sup> for SO<sub>2</sub>, 21.0 Tg yr<sup>-1</sup> for NO<sub>x</sub>, 27.7 Tg yr<sup>-1</sup> for VOC, 9.0 Tg yr<sup>-1</sup> for NH<sub>3</sub>, 10.8 Tg yr<sup>-1</sup> for PM<sub>10</sub>, and 6.9 Tg yr<sup>-1</sup> for PM<sub>2.5</sub>.

The constructed CREATEv3 (YR 2019) was compared with LTP (YR 2017) and KORUSv5 (YR 2016) as emission inventories previously used for air quality forecast models in China. First, the LTP (YR 2017) emissions were lower than those of CREATEv3 (YR 2019) for other pollutant emissions, excluding SO<sub>2</sub> and NH<sub>3</sub>. Additionally, KORUSv5 (YR 2016) emissions exceeded those of CREATEv3 (YR 2019) for all pollutants. Among them, a trend of decreasing emissions of SO<sub>2</sub>, NO<sub>x</sub>, VOC, and NH<sub>3</sub>, which affect the secondary production of fine particulate matter, was identified. When CREATEv3 (YR 2019) was used as input data for air quality modeling in Korea, the emissions of precursors were seemingly reduced, leading to an expected decrease in China's impact on fine particulate matter compared to that obtained using previous emissions data.

The results of comparing China's emissions by pollutant for each region using CREATEv3 (YR 2019) showed that the regions where the target pollutants were abundantly emitted significantly correlated with the major industries in the corresponding region. Additionally, to support the current air quality forecast model, CREATEv3 (YR 2019) was used to create CTM-ready emission data as input data for the air quality model. The gridded CTM-ready emissions and the regional distribution of CREATEv3 (YR 2019) showed slight differences owing to the application of temporal, spatial, and chemical speciation processes. However, they were similar overall. In addition, gridded CTM-ready emissions using the spatial allocation factor were found to consider the distribution of major emission sector concentration areas.

The use of CREATEv3 (YR 2019), which reflects recent changes in emissions in China, can potentially improve the accuracy of air quality forecasting models in Korea, leading to more reliable forecasts and supporting effective responses to changes in air quality. Future research is necessary to update the East Asian emission inventory to account for the latest emissions changes in these three countries following the COVID-19 pandemic.

#### Acknowledgements

This study was conducted with the support of the Air Quality Forecasting Center at the National Institute of Environmental Research under the Ministry of Environment (NIER-2022-01-02-072).

This research was supported by the FRIEND (Fine Particle Research Initiative in East Asia Considering National Differences) Project through the National Research Foundation of Korea (NRF), funded by the Ministry of Science and ICT (NRF-2020M3G1A1114621).

#### Authors' contributions

Contributed to the conception: SK, JK, HH, MJ, JL, SCH, OK, and JW. Development or design of the methodology: SK, JK, HH, MJ, JL, SCH, OK, and JW. Contributed to the acquisition of the data: JK, HH, MJ, JL, SCH, and OK. Contributed to the analysis and interpretation of the data: SK, JK, HH, MJ, JL, SCH, OK, and JW. Drafted and/or revised the article: SK, JK, HH, MJ, and JW. Approved the submitted version for publication: SK, HH, MJ, and JW.

#### Funding

This research was supported by the Air Quality Forecasting Center at the National Institute of Environmental Research under the Ministry of Environment (NIER-2022-01-02-072) and by the FRIEND (Fine Particle Research Initiative in East Asia Considering National Differences) Project through the National Research Foundation of Korea (NRF), funded by the Ministry of Science and ICT (NRF-2020M3G1A1114621), and by the Konkuk University's research support program for its faculty on sabbatical leave in 2022.

#### Availability of data and materials

Data will be made available from the authors upon reasonable request.

#### Declarations

##### Competing interests

The authors declare that they have no competing interests.

Received: 24 May 2023 Accepted: 30 August 2023

Published online: 06 December 2023

#### References

- Bae, H. S., Yu, S. H., & Kwon, H. Y. (2017). Fast data assimilation using Kernel tri-diagonal sparse matrix for performance improvement of air quality forecasting. *Journal of Korea Multimedia Society*, 20(2), 363–370. <https://doi.org/10.9717/krms.2017.20.2.3>
- CAMx (Comprehensive Air Quality Model with Extensions). (n.d.). From <https://www.camx.com/>
- Choi, J., Park, R. J., Lee, H. M., Lee, S., Jo, D. S., Jeong, J. I., Henze, D. K., Woo, J.-H., Ban, S.-J., Lee, M.-D., Lim, C.-S., Park, M.-K., Shin, H. J., Cho, S., Peterson, D., & Song, C.-K. (2019). Impacts of local vs. trans-boundary emissions from different sectors on PM<sub>2.5</sub> Exposure in South Korea During the KORUS-AQ Campaign. *Atmospheric Environment*, 203, 196–205. <https://doi.org/10.1016/j.atmosenv.2019.02.008>
- CMAQ (the Community MultiScale Air Quality). (n.d.). Website, from <https://www.epa.gov/cmaq>
- Crippa, M., Guizzardi, D., Butler, T., Keating, T., Wu, R., Kaminski, J., Kuenen, J., Kurokawa, J., Chatani, S., Morikawa, T., Pouliot, G., Racine, J., Moran, M. D., Klimont, Z., Manseau, P. M., Mashayekhi, R., Henderson, B. H., Smith, S. J., Suchyta, H., ... Foley, K. (2023). The HTAP\_v3 emission mosaic: Merging regional and global monthly emissions (2000–2018) to support air quality modelling and policies. *Earth System Science Data*, 15, 2667–2694. <https://doi.org/10.5194/essd-15-2667-2023>
- Jang, I. S., Lee, D. G., Yu, J. A., Hong, S. C., Son, J. S., Choi, J. Y. (2014). PM10 forecasting status and improvement measures. In *Proceedings of the Spring Meeting of KMS*, (in Korean with English abstract).
- Jang, Y., Lee, Y., Kim, J., Kim, Y., & Woo, J. H. (2020). Improvement China point source for improving bottom-up emission inventory. *Asia-Pacific Journal of Atmospheric Sciences*, 56, 107–118. <https://doi.org/10.1007/s13143-019-00115-y>

- Kim, J., Park, J., Hu, H., Crippa, M., Guizzardi, D., Chatani, S., ... & Woo, J. H. (2023). Long-term historical trends in air pollutant emissions in South Korea (2000–2018). *Asian Journal of Atmospheric Environment*, 17(1), 12.
- Lee, D., Kim, S., Kim, H., & Ngan, F. (2014). Retrospective air quality simulations of the TexAQS-II: Focused on emissions uncertainty. *Asian Journal of Atmospheric Environment*, 8(4), 212–224. <https://doi.org/10.5572/ajae.2014.8.4.212>
- Lee, K., Lee, S. H., & Kim, E. (2016). Assessment of global air quality reanalysis and its impact as chemical boundary conditions for a local pm modeling system. *Journal of Environmental Science International*, 25(7), 1029–1042.
- Li, M., & Jung, J. (2021). Assessing the development level of urbanization on the impact of air quality improvement: a case study of provinces and municipalities region. *China Journal of Environmental Policy and Administration*, 29(3), 77–111. <https://doi.org/10.15301/jepa.2021.29.3.77>
- Li, M., Liu, H., Geng, G., Hong, C., Liu, F., Song, Y., Tong, D., Zheng, B., Cui, H., Man, H., Zhang, Q., & He, K. (2017). Anthropogenic emission inventories in china: A review. *National Science Review*, 4(6), 834–866. <https://doi.org/10.1093/nsr/nwx150>
- MEIC (Multi-resolution Emission Inventory for China). (n.d.). From <http://meicmodel.org/?lang=en>
- NIER (National Institute of Environmental Research). (2017). *KORUS-AQ Rapid Science Synthesis Report, Incheon*.
- NIER (National Institute of Environmental Research). (2019). *Study on Comprehensive Evaluation and Improvement for the 4th LTP, 11–1480523–003834–01, Ministry of Environment*.
- NIER (National Institute of Environmental Research). (2021). *Development of Climate Pollutants Emission Inventory for East Asia(V), 11–1480523–004461–01, Ministry of Environment*.
- Simpson, I. J., Blake, D. R., Blake, N. J., Meinardi, S., Barletta, B., Hughes, S. C., Fleming, L. T., Crawford, J. H., Diskin, G. S., Emmons, L. K., Fried, A., Guo, H., Peterson, D. A., Wisthaler, A., Woo, J. H., Barré, J., Gaubert, B., Kim, J., Kim, M. J., ... Zeng, L. L. (2020). Characterization, sources and reactivity of volatile organic compounds (VOCs) in Seoul and surrounding regions during KORUS-AQ. *Elementa: Science of the Anthropocene*, 8, 37. <https://doi.org/10.1525/elementa.434>
- Sonntag, D. B., Baldauf, R. W., Yanca, C. A., & Fulper, C. R. (2014). Particulate matter speciation profiles for light-duty gasoline vehicles in the United States. *Journal of the Air & Waste Management Association*, 64(5), 529–545. <https://doi.org/10.1080/10962247.2013.870096>
- The University of North Carolina at Chapel Hill (UNC). (2020). *SMOKE v4.8.1 User's Manual*.
- Woo, J. H., Choi, K. C., Kim, H. K., Baek, B. H., Jang, M., Eum, J. H., Song, C. H., Ma, Y.-I., Sunwoo, Y., Chang, L.-S., & Yoo, S. H. (2012). Development of an anthropogenic emissions processing system for Asia using SMOKE. *Atmospheric Environment*, 58, 5–13. <https://doi.org/10.1016/j.atmosenv.2011.10.042>
- Woo, J. H., Kim, Y., Kim, H. K., Choi, K. C., Eum, J. H., Lee, J. B., Lim, J.-H., Kim, J., & Seong, M. (2020). Development of the CREATE Inventory in Support of Integrated Climate and Air Quality Modeling for Asia. *Sustainability*, 12(19), 7930. <https://doi.org/10.3390/su12197930>
- Yarwood, G., Jung, J., Whitten, G.Z., Heo, G., Mellberg, J., & Estes, M. (2010). Updates to the carbon bond mechanism for version 6 (CB6). In *9th Annual CMAS Conference* (pp. 11–13). Chapel Hill
- Zheng, B., Zhang, Q., Geng, G., Chen, C., Shi, Q., Cui, M., Lei, Y., & He, K. (2021). Changes in China's anthropogenic emissions and air quality during the COVID-19 pandemic in 2020. *Earth System Science Data*, 13(6), 2895–2907. <https://doi.org/10.5194/essd-13-2895-2021>

## Publisher's Note

Springer Nature remains neutral with regard to jurisdictional claims in published maps and institutional affiliations.